EJAC
Eurasian Journal of Analytical Chemistry

Eurasian J. Anal. Chem. 4(3): 226-233, 2009

More Experimental and Analytical Evidence of the New Intensity Formula in Optical Emission Spectroscopy

Bo Thelin[1]

Solarphotonics HB, Granitvägen 12 B, 752 43 Uppsala , Sweden

Received: *08 August 2009;* ***Accepted:*** *25 September 2009*

Abstract

This paper is a review of different methods supporting a new intensity formula in optical emission spectroscopy. Three independent experimental and analytical methods have been developed which strongly support this new formula. Different light sources have also been used in this work. A new theory has also been presented which strongly verify the new formula. Support is also given from experimental data of many old and new physical and analytical methods in the literature. In this paper the different parts of the new formula are examined and verified from many papers in the literature..

Keywords:

Arc, DC, Hollow cathode and laser excitation, inductively coupled plasma, γ-ray, X-ray, UV, optical and IR-Spectroscopy, Astrophysics, Analytical methods, Photoluminiscence, Electroluminiscence, Piezoelectric Photothermal Spectroscopy, Surface Photovoltage Spectroscopy

1. Introduction

According to a new theory the intensity I is given by

$$I = C\ \lambda^{-2}(exp(- J/ k T)) / (exp (h \nu /k T) - 1) \quad (1)$$

J is here the ionization energy, and C is a factor given by transition probabilities, number densities and sample properties. λ and ν are here the wavelength and frequency of the atomic spectral line. This means that the new intensity formula consists of 4 parts: the C-factor, λ^{-2}-part, the J-dependence exp(-J / k T) and the Planck factor 1/((exp(h ν / k T) - 1) about this formula. We have developed three methods of analyses: the fluctuation analysis.

The first method which was developed supporting the intensity formula with an exponential hν term is the fluctuation method. In this method concerns the study of spectral line intensity ratio fluctuations in Ref.1. By forming the ratio between the intensities of two simultaneously measured lines from the same sample and by using logarithmic differentiation, we obtain the following expression:

$$d (I^a_{mn} / I^b_{kl}) / (I^a_{mn} / I^b_{kl}) = d (C^a_{mn} / C^b_{kl}) / (C^a_{mn} / C^b_{kl}) + (1 /k T)(d T / T) D (E) \quad (2)$$

where $D (E) = J^a - J^b + h \nu^a_{mn} - h \nu^b_{kl}$. Mathematically this formula is a straight line, which can be seen in Fig.1 of Ref.1 from a hollow cathode experiment. In this figure fluctuation data R versus $D(E)= J^a - J^b + E^a_{mn} - E^b_{kl}$ (difference of ionization energy plus photon energy) were used from fifteen steel samples in a hollow cathode lamp. Seventeen elements were studied in

[1] **Phone:** 4618507253 **Fax:** 4618507253 **E-mail:** btn602003@yahoo.se
ISSN: 1306-3057

this graph giving a correlation coefficient of 0.90. In this paper similar graphs were obtained with an ICP –light source and many earlier papers by us were referred to.

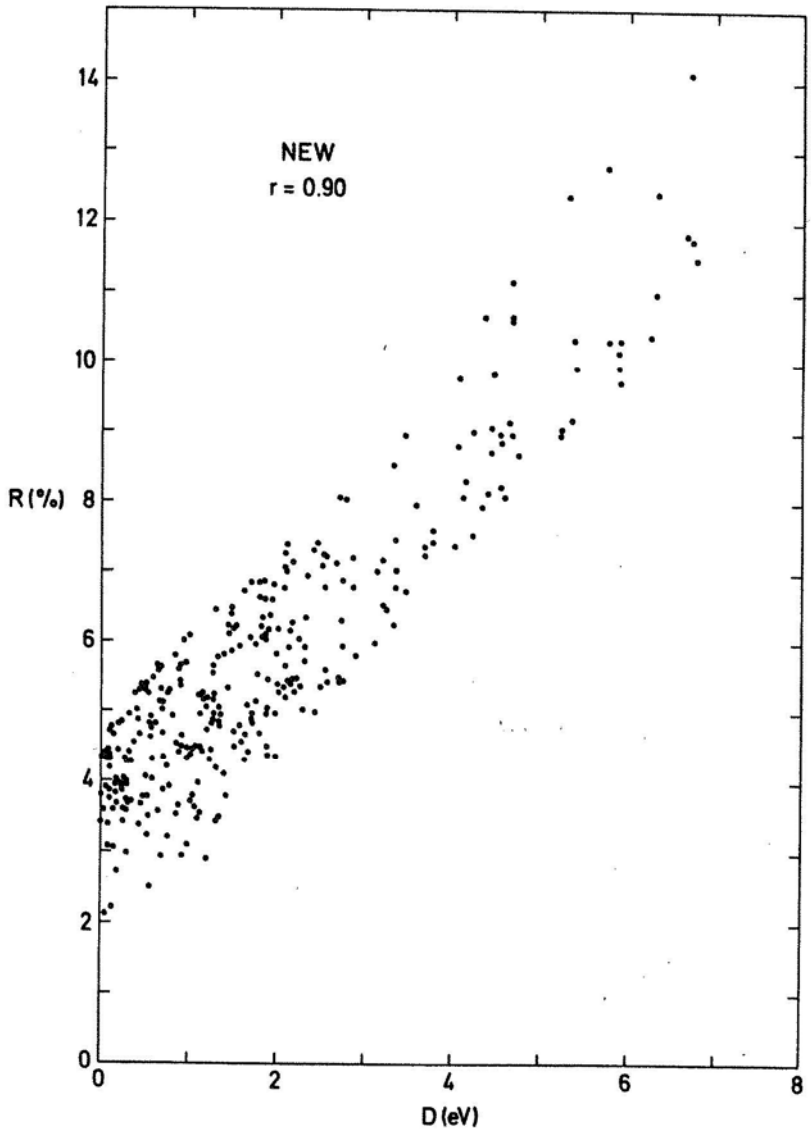

Fig 1. Plot of fluctuation data R versus D (E) = J^a - J^b + E^a_{mn} - E^b_{kl} (difference of ionization energy plus photon energy) from fifteen steel samples used in a hollow cathode lamp. Seventeen elements were studied in this graph. (Reproduction from Ref.1)

A second method was also developed in Ref.1 and in Ref.2 by studying absolute intensity of spectral lines. It is also possible to obtain linear relationships by studying logarithmic expression:

$$\ln (I \lambda^2) = -(h\nu/kT)(1 + (kT/h\nu)\ln (1- \exp(-h\nu/kT))) \quad (3)$$

which was developed from Equation 1. This investigation was based on NBS intensity tables on arc measurements. The points in this graph represent the mean values of many spectral lines in a small wavelength interval. Such a graph is shown in p.819 of Ref.2, which is a graph of C(II) (ions) showing linearity over 25 eV. This is indeed a remarkable result with a correlation coefficient r = -0.87. Corresponding result for C(I) was r= -0.97 over 14eV.These results are a very strong evidence of Equation 1.

A third method of analysis has been developed concerning the detection limits of ionic spectral lines in an inductively coupled plasma experiment. A table of transition probabilities of spectral lines in an arc experiment was also used in Ref.3. The results from that analysis of detection limit data are very consistent with the new spectral line expression of Equation 1.

The new theory in Ref.4 is in accordance with Equation 1 and is based on first principles of quantum physics, electrodynamics and statistical physics. The theory is strongly supported by experimental evidence.

2. Further literature evidence

New material found in the literature, done by others in the past, show data which has shown to support our intensity formula too. These findings together with our earlier works prove to be another strong evidence of Equation 1. It is frequent in the literature to find papers having data which support the new intensity formula. Many new papers from the Asian countries include data from different experimental methods which support the new formula. Some of these papers are shown here. We will now study the different parts of Equation 1 and show support in the literature of these parts.

3. The exp (- J / k T) dependence

3.1. Inductively coupled plasma

In a paper by Blades et al in Ref.5 an ICP- temperature investigation was carried out for different elements on different heights of the ICP-plasma. A straight line was obtained, where the heights of different spectral lines (peak values) from different elements were plotted versus the normal temperature. According to this graph the I(max) from these lines are inversely proportional to the heights(h) of the lines. From that graph (Fig (19, p.861) in this reference) it is possible to plot the height versus (J + h ν), which is linear and shows a direct proportionality between height and (J +hν) and is shown in Fig 2. Because I(max) is inversely proportional to h (height), means that I(max) is inversely proportional to (J + h ν) which is in accordance to the Equation 1.

In Ref.6 fundamental characteristics concerning plasma related matrix effects were studied. The intensity from the plasma were here plotted versus the the first ionization energy of the elements studied. The intensity was here decreasing with increasing ionization energy according to Equation 1.

3.2. Laser experiment

In another experiment Ref.7 (Figs 9.7, 9.11, 9.12 and 9.13 p.735, 744 and 745) using a neodym laser at different pulse times in combination with a argon flash equipment. The intensity of that experiment was plotted versus the argon pressure, where the intensity is inversely proportional to the pressure. The pressure is also inversely proportional to the ionization to the ionization grade, which according to Saha standard equation is proportional to exp(-J/kT). J is here the ionization potential. This means that the intensity is proportional to exp(-J/kT), according to Equation 1.

3.3. Different gas plasmas

The term exp (-J / k T) in Equation 1 is clearly demonstrated in Ref. 8 (Figs 3.12 , 3.13a and 3.13b p.100-102), where relationships between absolute and relative line intensities versus temperature for different plasmas of (Ar , N_2 and O_2). In these graphs absolute and relative intensities were plotted versus measured temperature of a number of atomic spectral lines. These graphs go to a maximum, which is higher for elements with lower (J + hν)-values according to Equation 1.In the same reference similar graphs were studied for ion spectral

lines of the same gases. The results were the same as for the atomic spectral lines; higher intensity for lower (J + hν)-values. Ionic spectral lines do follow the similar J-dependence as the atomic spectral lines of Equation 1, which is examined in detail in Ref. 3.

4. The Planck factor 1/ (exp (h ν / k T) -1)

According to literature in Ref.9 (Figs 15-1 and 15-2 on p.451) the contributions of continuous spectrum is mainly dominating in the high temperature range while the contributions from the discrete emissions are mainly dominating in the lover temperature range.

4.1. Astrophysics

Both continuous and discrete spectrum have the same appearance which is seen in Ref.10, where the hydrogen Balmer absorption lines of the sun and the stars have the same appearance as the continuous spectrum. This appearance is the well known Planck curve with steeper low wavelength side and a slower high wavelength side. The wavelength of the intensity maximum of the continuous and discrete spectrum seem to be the same which is in accordance to Equation 1 and the new theory, where the Planck factor is a part of the new intensity formula. These facts are clearly seen in many Planck curves in Ref.10 from different kinds of stars. The normalized flux is here proportional to the emissions from the continuous and discrete spectrum.

4.2. Different gas plasmas

Another evidence of Equation 1 is also seen in experiments where temperature calculations in relation to absolute and relative line intensities of argon, nitrogen and oxygen were carried out. In Ref.8 (Figs 3.12 , 3.13a and 3.13b p.100-102) such an intensity versus temperature graph has the appearance of a maximum. This maximum is higher for higher wavelength, which is in accordance with the hν-dependent Planck factor of Equation 1.

4.3. X-ray, γ-radiation and IR-experiments

Similar intensity versus wavelength profile as in the optical experiments above has also been observed in the X-ray field which is studied in Ref.11 (Fig 238 p.444 and Fig 248 p.457).In this experiments fast electrons been accelerated against a metal electrode. In this experiment the X-ray emission spectral lines following the usual optical Planck factor profile in our formula. Planck factor profiles are also observed in the line spectrum of the γ-radiation from the decay of a Ra preparation (Ref.12) (Fig 19 p.18) and in the IR-region(0.2-2μm) from a 1000W-Hg-lamp (Ref.13) (Figs 2-42 and 44 p.2-51 and 52).In the IR-experiment the light was taken out perpendicular to the main axis to obtain lower background.

4.4. FTIR-spectra

In Ref.14 (Figs 3 and 4, p.1534) FTIR spectra (Fourier transform infrared) is shown in the infrared region on SiO-CH films. The envelope of the molecule bands CH_3 and CH_2 show a clear Planck factor structure emanating from discrete energy levels in the molecules. As Equation 1 originates from atomic spectra, it is plausible to believe that this photon distribution (the most probable according to Ref.4**)** also deals with molecules. This photon distribution is the same between emission and absorption, with the only difference in the C-factor.

This means that the new intensity formula seems to be applicable in the γ, X-ray, optical and the IR-regions. In those examples the wavelength of the intensity maximum of the discrete emissions seems to be equal to the intensity maximum of the continuum, which supports the Planck factor of our formula.

4.5. The LED-lamps, Photoluminiscence and Electroluminiscence

Planck factor is also strongly supported by the intensity profile $I = f(\lambda)$ of the LED-lamps .These lamps are working at low temperature as in Ref.15 (Fig 3, p.5087) and Ref.16 (Fig 6b, p.8267). These curves were coming from experiments in room temperature and far below (26-200K) from photoluminisscence FL-experiments.

In Ref.17 (Figs 7 and 8, p.7431) photoluminescence spectra for EU-doped titania nano-particles is at room temperature. These graphs show that the wavelength of the intensity maximum of the continuous and discrete emissions seems to be the same.

Ref.18 (Fig 5, p.1299) show similar intensity-wavelength profile (Planck factor) between both electroluminescence and photoluminescence spectra. In this paper electrons were injected into an organic field- effect transistor with Au electrodes. An electric AC-field was used to obtain electroluminescence. To obtain photoluminescence here an UV LED on tetracene thin film, was used.

In Ref.19 (Fig 5, p.1268) photoluminescence spectra is shown for $Ir(ppy)_3$ in CBS at 5K. Intensity-wavelength graphs for 0-0, 0-1 and 0-2 phonon bands were shown and show a Planck factor profile when integrated with all the bands. This Planck factor profile originates probably from Equation 1 as the temperature here was very low. In this paper the occupation number of the effective phonon modes seems to be very similar to the Planck factor.

In Ref.20 Fig(2-4, p.542) is photoluminescence spectra shown for submicron-sized ZnO crystals, registrated in the temperature range 8-300K. These spectra show a clear Planck factor profile, when looking at the envelope of the discrete emissions.

Similar results have been observed in Ref.21 (Fig 2, p.417), where polyfluorene films were used. The deep minima indicate that only discrete emissions were registrated, which support Equation 1.

4.6. Laser experiment

Ref.22 (Fig 3, p.6791) shows an optical spectrum (power versus wavelength) from a laser experiment (laser breakdown pulses) over the whole visible spectrum. In this experiment laser breakdown pulses were generated in tap water. The envelope of the two peaks follows a Planck profile and the wavelength maxima of the continuous and the discrete emissions seem to be the same according to Equation 1.

5. The C-factor

5.1. Laser experiment

In Fig (9.9, p.737 of Ref.7 the breakdown pressure is plotted versus ionization energy for some atomic and molecular gases. In this investigation the laser power was fixed. The C-factor includes the number densities of a gas, which means the pressure in this experiment. In this experiment the pressure is proportional to the ionization energy. This fact is in accordance to Equation 1 because the C-factor can be expressed as approximately

$$C = I \quad \lambda^2 \exp((\ J + h\,\nu) / k\,T\ ) \tag{4}$$

6. λ-Dependence

6.1. X-ray experiments

This dependence has been studied earlier Ref.23 (Fig 2-9, p.93) and Ref.24 (Fig 12, p.349) in the X-ray field, where

$$I(\lambda) = \text{const}\ \lambda^{-2} \quad (5)$$

For the X-ray emissions. In this wavelength region the hν-value is very big which makes the Planck factor around 1. If k T ≈ h ν ,then Equation 5 is achieved from Equation 1.For a specific element this expression is in accordance with Equation 1.

7. Discussion

The new intensity formula has shown to be applicable to many light sources at different experimental conditions and temperatures.

The spectral line intensity ratio fluctuation analysis of Ref.1 is a very sophisticated method of sorting the correct formula, where questions concerning photon efficiency versus wavelength for spectrometer systems, can be eliminated.

In Ref.2 the absolute intensity method shows linearity over 25 eV for C (l l) – lines. This is impossible to achieve without a correct intensity formula. Deviations caused by photon efficiency versus wavelength for spectrometer systems are here very small in these graphs. The most dominant linearity factor is a correct exponent in the intensity formula.

Fig.2 is a strong support of Equation 1 and J – dependence from the heights in and ICP-plasma. Many different elements were used which gave a linear relationship.

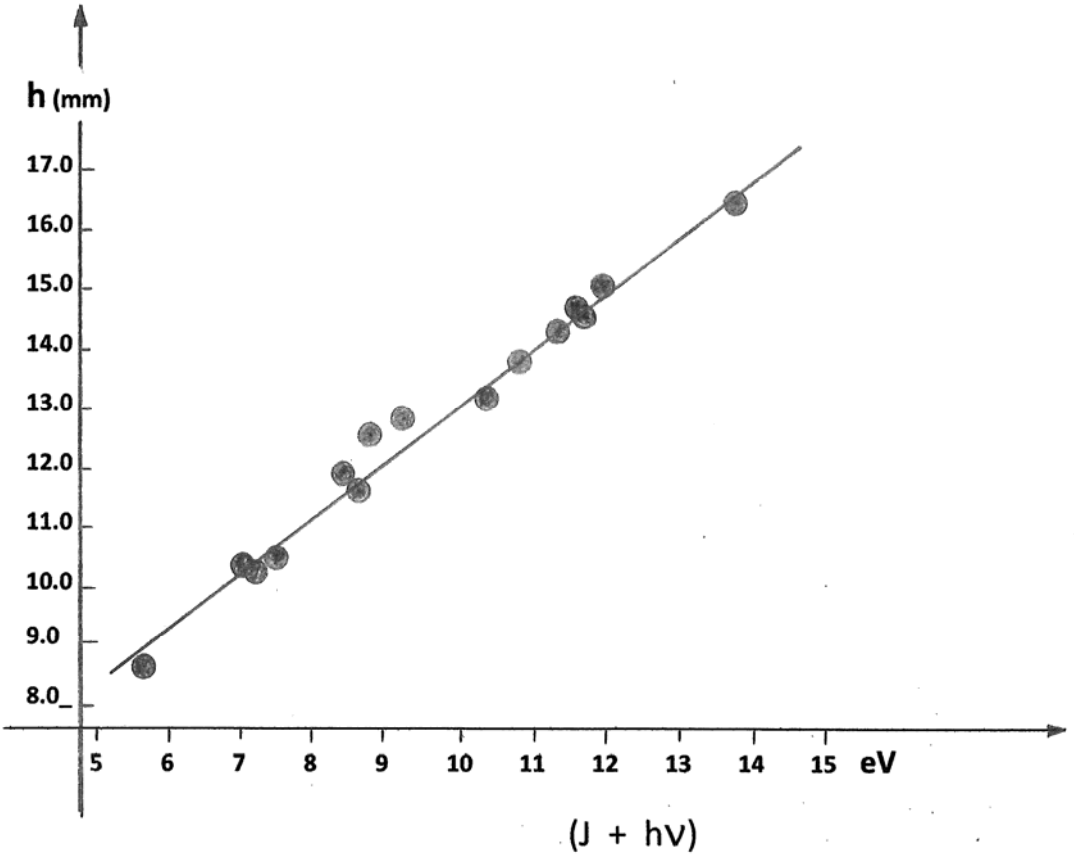

Fig 2. This graph shows a linear relationship between height in the ICP–plasma and J + hν for different elements studied

Planck curves of Ref.10 are strong evidence of the Planck factor in Equation 1, because the wavelength of the intensity maximum for the continuous-and absorption lines (Balmer) seem to be the same. Many of the Asian papers work at very low temperature are also a very strong proof of this factor, because in these temperature intervals only discrete transitions are

dominating. In many of these graphs there are deep minima between the peaks. These facts verify that there are only discrete emissions here, which support Equation 1. According to the theoretical paper Ref.4, the Planck factor originates from the most probable photon distribution. It is very likely to suggest that this factor concerns both atomic and molecular spectra in all wavelength regions, which has also been observed.

Acknowledgement

I express a big gratitude to my friend and collegue Dr. Sten Yngströmat the Swedish Institute of Space Physics for inspiring and skillful cooperation during many years. I also gratitude Prof. Bengt Hultqvist at Swedish Institute of Space Physics for his encouraging support of this work.

References

1. Yngström S, Thelin B (1990) Evidence of a New Spectral Line Intensity Formula for Optical Emission. Appl Spectrosc. 44: 1566.
2. Thelin B (1990) An Expression for Spectral Line Intensity Data. Appl Spectrosc 44: 818.
3. Yngström S (1994) Relationship between Detection Limits and Energy Quantities in Atomic Emission Spectrometry. Appl Spectrosc 48 (5): 587.
4. Yngström S (1994) Theory of Atomic Spectral Emission Intensity. Int J Theor Phys 33 (7): 1479.
5. Blades M W and Horlick M G (1981) Interference From Easily Ionizable Element Matrices in Inductively Coupled Plasma Emission Spectrometry--A Spatial Study.Spectrochimica Acta 36B (9): 881-900
6. Chan G C and Hieftje G M (2009) Fundamental characteristics of plasma-related matrixeffect cross-over points in inductively coupled plasma-atomic emission spectrometry. J Anal At Spectrom 24: 439–450.
7. Meek J M, Cragg J D (1978) Electrical Breakdown of gases, John Wiley&Sons, Chichester, New York, Brisbane, Toronto.
8. Dresvin S V (1977) Physics and Technology of Low-Temperature Plasmas, The Iowa State University Press, Ames.
9. Penner S S (1959) Quantitative Molecular Spectroscopy and Gas Emissivities, Addison-Westley Publishing Company,Inc., Massachusetts , USA, London England.
10. Silva D R, Cornell M E (1992) A New Library of Stellar Optical Spectra, Astrophys J Suppl Ser 81 (2): 865
11. Siegbahn M (1931) Spekroskopie der Röntgenstrahlen, Verlag von Julius Springer, Berlin.
12. Schaffs W (1957) Handbuch der Physik, Erzeugung von Röntgenstrahlen, Springer-Verlag, Berlin.
13. Suits H (1989) The Infrared Handbook, Environmental Research Institute of Michigan,Office of Naval Research,Department of the Navy, Washington, DC.
14. Huang C H, Huang H L, Hung C I, Wang N F, Wang Y H, Houng M P (2008) Bond Structure in Porous SiOCH Low-k Film Fabricated by Ultaviolett Irradiation. Jpn J Appl Phys 47 (3):1532.

15. Li F, Son D I, Kim T W, Dong W, Kim Y H (2008) Optical Properties of Self-Assembled ZnO Nanocrystals Embedded in a p-Phenylene Biphenyltetracarboximide Polymide Layer. Jpn J Appl Phys 47 (6): 5086.
16. Choi J, Jhin J, Yang S, Baek J, Lee J, Byun D (2008) Effect of Patterned Ion-Implanted Sapphire on Ultraviolet Light-Emitting Diodes. Jpn J Appl Phys 47 (11): 8265.
17. Tsuboi T, Setiawati E, Kawano K (2008) Spectroscopy Study on the Location and Distribution of Eu^{3+} Ions in TiO_2 Nanoparticles. Jpn J Appl Phys 47 (9): 7428
18. Ohshima Y, Kohn H, Lim E, Manaka T, Iwamoto M (2008) Observation of Electron Injection into Organic Field Effect Transition with Au Electodes using Electroluminiscence under AC Electric Field. Jpn J Appl Phys 47(2):1297.
19. Tsuboi T, Aljaroudi N (2008) Electronic Relaxation Processes in the T state of Phosphorescent fac-Trisne(2-phenylpyridine)Iridium Molecule in $4,4^1$-N,N^1-Dicarbazole-biphenyl Host. Jpn J Appl Phys 47(2): 1266.
20. Htay M T, Itoh M, Hashmoto Y, Ito K (2008) Photoluminiscence Properties and Morphologies of Submicron-Sized ZnO Crystals Prepared by Ultrasonic Spray Pyrolysis. Jpn J Appl Phys 47(1): 541.
21. Tanigaki N, Heck C, Mizokuro T, Minato H, Misaki M, Yoshida Y, Azumi R (2008) Dope-Dye Orientation Relative to Oriented Polyfluorene Host Film. Jpn J Appl Phys 47(1): 416
22. Chekhovskiy A, Toshiyoshi H (2008) The Use of Laser Burst for Volumetric Display Inside Transparent Liquid. Jpn J Appl Phys 47(8): 6790.
23. Comton A H, Allison S K (1935) X-rays in Theory and Experiment,D. van Nostrand Company,Inc. Princeton, New Jersey, Toronto, London.
24. S.Flügge (1957) Handbuch der Physik, Springer-Verlag, Berlin, Göttingen, Heidelberg.